ACS APPLIED MATERIALS & INTERFACES

Research Article

www.acsami.org

Significant Promotion Effect of Mo Additive on a Novel Ce−Zr Mixed Oxide Catalyst for the Selective Catalytic Reduction of NO_x with NH_3

Shipeng Ding, Fudong Liu,*,† Xiaoyan Shi, Kuo Liu, Zhihua Lian, Lijuan Xie, and Hong He*

State Key Joint Laboratory of Environment Simulation and Pollution Control, Research Center for Eco-Environmental Sciences, Chinese Academy of Sciences, 18 Shuangqing Road, Haidian District, Beijing 100085, P. R. China

Supporting Information

ABSTRACT: A novel Mo-promoted Ce−Zr mixed oxide catalyst prepared by a homogeneous precipitation method was used for the selective catalytic reduction (SCR) of NO_x with NH_3. The optimal catalyst showed high NH_3-SCR activity, SO_2/H_2O durability, and thermal stability under test conditions. The addition of Mo inhibited growth of the CeO_2 particle size, improved the redox ability, and increased the amount of surface acidity, especially the Lewis acidity, all of which were favorable for the excellent NH_3-SCR performance. It is believed that the catalyst is promising for the removal of NO_x from diesel engine exhaust.

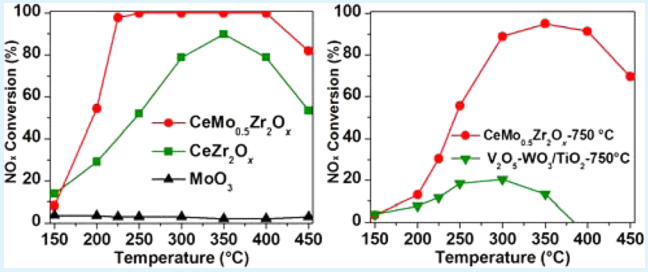

KEYWORDS: *selective catalytic reduction, nitrogen oxides, diesel engine exhaust, thermal stability, Ce−Zr mixed oxide*

1. INTRODUCTION

Nitrogen oxides (NO_x) emitted from stationary and mobile sources have been major atmospheric pollutants. The selective catalytic reduction (SCR) of NO_x with NH_3 or urea has been extensively studied as one of the most effective methods to remove NO_x, and the most widely used commercial catalyst is $V_2O_5-WO_3/TiO_2$.[1−4] However, there are still some inevitable disadvantages with this catalyst system, such as the toxicity of vanadium pentoxide, narrow operation temperature window, and high conversion of SO_2 to SO_3 at high temperature.[5] Therefore, it is desirable to develop a novel NH_3-SCR catalyst that can substitute for the conventional V-based catalyst in recent years.

Cerium oxide (CeO_2) as one of the most abundant rare-earth oxides has attracted much interest over the past decades in many catalytic reactions such as carbon monoxide oxidation, water−gas shift, nitric oxide reduction, and reforming reactions.[6−8] However, pure CeO_2 shows poor thermal stability and is susceptible sintering at high temperature.[9] It has been reported that the addition of ZrO_2 to CeO_2 leads to improvement in the oxygen storage capacity and thermal stability.[10,11] Ce−Zr mixed oxide combines the highly refractory property of ZrO_2 with the oxygen storage capacity of CeO_2, which can be used as a catalyst or support for NH_3-SCR of NO_x. It was found that nickel and sulfate modification increased the strength of Lewis acid sites and enhanced the NH_3 adsorption capacity, all of which were beneficial for improvement of the activity and selectivity of Ce−Zr catalyst.[12] It was also believed that NiO on the CeO_2 nanorods played an important role for enhancement of the NH_3-SCR activity because of the higher concentration of Ce^{3+}, larger amount of active O_α, lower amount of energy required for oxygen vacancy distortion, and strong interaction between NO and NH_3.[13] The experimental and kinetic model results indicated that the $MnO_x(0.6)/Ce_{0.5}Zr_{0.5}O_2$ catalyst showed high NO conversion and N_2 selectivity at low temperatures, and the apparent activation energy of the NH_3-SCR reaction on $MnO_x(0.6)/Ce_{0.5}Zr_{0.5}O_2$ (18 kJ/mol) was lower than that on MnO_x/TiO_2 (38 kJ/mol).[14] A WO_3/CeO_2-ZrO_2 catalyst annealed in air at 800 °C for 1 h still showed high NH_3-SCR activity.[15] The three-dimensional ordered macroporous (3DOM) $Ce_{0.75}Zr_{0.2}M_{0.05}O_{2-\delta}$ (M = Fe, Mn, Co) synthesized by a colloidal template method also exhibited good activity for NH_3-SCR of NO_x; the characterization results showed that the dopants were effectively doped into the Ce−Zr oxide solid solution and a strong synergistic effect existed between the dopants and Ce−Zr oxide, all of which were beneficial for improvement of the NH_3-SCR activity.[16] It was also found that the morphology of $CeZrO_x$ had a remarkable effect on the performance of the MnO_x/CeO_2-ZrO_2 catalyst for the NH_3-SCR reaction, and MnO_x/CeO_2-ZrO_2 nanorods showed activity superior to that of nanotubes and nanopolyhedra.[17] $Ce_{0.75}Zr_{0.25}O_2-PO_4^{3-}$ catalyst prepared by impregnating phosphates on $Ce_{0.75}Zr_{0.25}O_2$ still presented high SCR activity at 300−400 °C after hydrothermal aging at 760 °C for 48 h, which might result from the fact that phosphates improved NH_3 adsorption and suppressed the unselective oxidation of NH_3 at high temperatures.[18] Although catalysts containing CeO_2-ZrO_2 oxide, such as WO_3/CeO_2-ZrO_2[15], $MnO_x/Ce_{0.5}Zr_{0.5}O_2$[14], $Ce_{0.75}Zr_{0.25}O_2-PO_4^{3-}$ and Ni-modified Ce−Zr

Received: January 21, 2015
Accepted: April 20, 2015
Published: April 20, 2015

DOI: 10.1021/acsami.5b00636
ACS Appl. Mater. Interfaces 2015, 7, 9497−9506

oxide,[18] have been used toward NH_3-SCR of NO in recent years, the promotional effect of Mo addition on the NH_3-SCR activity over CeO_2−ZrO_2 and the thermal stability of $CeMo_{0.5}Zr_2O_x$ catalyst have never been investigated in recent publications. In addition, MoO_3 is widely used as a stabilizer and a promoter to improve the activity, mechanical, and structural properties of a V_2O_5/TiO_2 catalyst for NH_3-SCR prcocess.[19−21] It was also found that the addition of MoO_3 promoted the adsorption and activation of NH_3, which was conducive to improvement of the NH_3-SCR activity of a MoO_3-doped Ce/TiO_2 catalyst.[22]

In order to take full advantage of the high NH_3-SCR activity and thermal stability of Ce−Zr mixed oxide and promoting effect of MoO_3, in the present work, a series of novel Mo-promoted Ce−Zr catalysts was prepared by a homogeneous precipitation method and were applied to NH_3-SCR of NO_x. The catalyst showed high SCR activity, SO_2/H_2O durability, and thermal stability under test conditions. The structure, redox ability, and acidity of the catalyst were characterized using different techniques. The promotional effect of Mo species and the NH_3-SCR reaction mechanism over the catalyst were fully discussed. The catalyst is quite promising for NO_x emission control from diesel engine exhaust.

2. EXPERIMENTAL SECTION

2.1. Catalyst Preparation and Activity Test. The catalysts were prepared by a novel and facile homogeneous precipitation method using urea as the precipitator.[23] All chemicals used were of analytical grade. The aqueous solution of $Ce(NO_3)_3{\cdot}6H_2O$, $Zr(NO_3)_4{\cdot}5H_2O$, and $(NH_4)_6Mo_7O_{24}{\cdot}4H_2O$ was mixed with the required molar ratio. An excessive urea aqueous solution was then added to the mixed solution. The solution was heated to 90 °C and continuously stirred for 12 h. The pH variation of the mixed solution during the homogeneous precipitation process is shown in Figure S1 in the Supporting Information (SI). The initial pH of the mixed solution, which was measured by a pH meter (Sartorius PB-10), was about 1.0 because of hydrolysis of the precursors. However, as the preparation time increased from 1.0 to 4.0 h, a substantial amount of precipitate was formed and the pH was greatly increased from 1.0 to 7.0 probably because of the decomposition of urea. After filtration and washing with deionized water, the resulting precipitate was dried at 100 °C overnight and subsequently calcined at 500 °C for 3 h in air. The bulk molar ratios of Ce:Mo:Zr in the $CeMo_aZr_2O_x$ series of catalysts were analyzed by an inductively coupled plasma instrument (OPTMIA 2000DV). As shown in Table S1 in the SI, the actual proportions of Ce:Mo:Zr in the bulk were not consistent with the designed ones, indicating that not all of the ions precipitated in the process of homogeneous precipitation. In addition, the distribution of Zr, Ce, and Mo derived from scanning electron microscopy−energy-dispersive X-ray (SEM−EDX; Hitachi S-3000N) over $CeMo_{0.5}Zr_2O_x$ catalyst prepared by homogeneous precipitation was presented in Figure S2 in the SI. Zr exhibited a slightly poor dispersion; however, the Ce and Mo species were homogeneously dispersed on the surface of the catalyst. The catalysts were also calcined at desired temperatures (500, 550, 600, 650, 700, and 750 °C) for 8 h to test the thermal stability. In addition, the $CeMo_{0.5}Zr_2O_x$ catalysts were also hydrothermally aged at 700 and 760 °C for 48 h to evaluate the hydrothermal stability. The calcined samples were crushed and sieved to 40−60 mesh for the activity test. The catalysts were denoted as $CeMo_aZr_bO_x$, where a (a = 0, 0.1, 0.5, 1.0, 1.5) represented the molar ratio of Mo:Ce and b (b = 0.5, 1.0, 2.0, 4.0) indicated the molar ratio of Zr:Ce. The $CeMo_{0.5}Zr_2O_x$ catalysts calcined at different temperatures for 8 h were denoted as $CeMo_{0.5}Zr_2O_x$-t, where t represented the calcination temperature in degrees Celsius. For comparison, a conventional V_2O_5−WO_3/TiO_2 catalyst with 3 wt % (or 1 wt %) V_2O_5 and 10 wt % WO_3 was also prepared using the conventional impregnation method. NH_4VO_3 and $(NH_4)_{10}W_{12}O_{41}$ were used as sources of V and W, respectively. After impregnation, the excess H_2O was removed in a rotary evaporator at 60 °C. The sample was dried at 100 °C overnight and subsequently calcined at desired temperatures for 8 h in air.

The NH_3-SCR activity tests were carried out in a fixed-bed quartz tube reactor at atmospheric pressure. The weights of the catalysts employed were 1.10 g of $CeZr_2O_x$, 0.95 g of $CeMo_{0.1}Zr_2O_x$, 0.75 g of $CeMo_{0.5}Zr_2O_x$, 0.67 g of $CeMo_{1.0}Zr_2O_x$, and 0.56 g of $CeMo_{1.5}Zr_2O_x$ to maintain the gas hourly space velocity (GHSV) at 50000 h^{-1} over various catalysts. The reaction gas contained 500 ppm of NO (or [NO] = 250 ppm; [NO_2] = 250 ppm), 500 ppm of NH_3, 5 vol % O_2, N_2 balance, and 500 mL/min flow rate. Furthermore, 5 vol % H_2O or 100 ppm of SO_2 (or 500 ppm of SO_2) was introduced to the reaction gas to test the poisoning effect of H_2O/SO_2 on NO_x conversion over the $CeMo_{0.5}Zr_2O_x$ catalyst. The effluent gas was continuously analyzed by a Fourier transform infrared (FTIR) spectrometer (Nicolet Nexus 670) equipped with a heated, low-volume multiple-path gas cell (2 m). The FTIR spectra were collected after 1 h when the SCR reaction reached a steady state. NO_x conversion and N_2 selectivity were calculated as follows:

$$NO_x\ \text{conversion} = \left(1 - \frac{[NO]_{out} + [NO_2]_{out}}{[NO]_{in} + [NO_2]_{in}}\right) \times 100\%$$

$$N_2\ \text{selectivity} = \frac{[NO]_{in} + [NH_3]_{in} - [NO_2]_{out} - 2[N_2O]_{out}}{[NO]_{in} + [NH_3]_{in}} \times 100\%$$

2.2. Characterization. The N_2 adsorption−desorption isotherms over catalysts were obtained at 77 K using a Quantachrome Autosorb-1C instrument. Prior to N_2 physisorption, all samples were degassed in a vacuum at 300 °C for 5 h. The surface areas were determined by a Brunauer−Emmett−Teller (BET) equation in the 0.05−0.35 partial pressure range. Pore volumes were determined by the Barrett−Joyner−Halenda (BJH) method from the desorption branches of the isotherms.

Powder X-ray diffraction (XRD) measurements of the catalysts were carried out on a computerized PANalytical X'Pert Pro diffractometer with Cu Kα (λ = 0.15406 nm) radiation. The data of 2θ from 20 to 80° were collected at 8°/min with a step size of 0.07°.

Visible Raman spectra of the catalysts were collected at room temperature on a Spex 1877 D Triplemate spectrograph with a spectral resolution of 2 cm^{-1}. A 532 nm diode-pumped solid-state semiconductor laser was used as the excitation source with a power output of 30 mW. The time for recording each spectrum was 10 s.

The H_2-TPR (temperature-programmed reduction) experiments were carried out on a Micromeritics AutoChem 2920 chemisorption analyzer. In a typical measurement, 100 mg of the catalyst was first pretreated in a flow of 20 vol % O_2/N_2 (50 mL/min) at 400 °C for 0.5 h and then cooled to the room temperature (30 °C) followed by Ar purging for 0.5 h. Then the temperature was linearly raised at 10 °C/min from 30 to 700 °C in a flow of 10 vol % H_2/Ar (30 mL/min). H_2 consumption was monitored by a thermal conductivity detector.

NH_3-TPD (temperature-programmed decomposition) together with NO-TPD was also conducted on a Micromeritics AutoChem 2920 chemisorption analyzer, equipped with a quadrupole mass spectrometer (MKS Cirrus) to monitor the signals of NH_3 (m/z 17) and NO (m/z 30). Prior to TPD experiments, the 100 mg samples were pretreated at 400 °C in a flow of 20 vol % O_2/N_2 for 0.5 h and cooled to room temperature. Then the samples were exposed to a flow of NH_3 or NO + O_2 for 1.0 h. Finally, the temperature was raised to 600 °C in an Ar flow at the rate of 10 °C/min.

The in situ diffuse-reflectance infrared Fourier transform spectroscopy (DRIFTS) experiments were carried out on an FTIR spectrometer (Nicolet Nexus 670) equipped with a smart collector and an MCT/A detector cooled by liquid nitrogen. Prior to each experiment, the sample was pretreated at 400 °C for 0.5 h in 20 vol % O_2/N_2 and then cooled to 200 °C. The background spectrum was collected in flowing N_2 and automatically subtracted from the sample spectrum. The reaction conditions were as follows: 500 ppm of NH_3,

DOI: 10.1021/acsami.5b00636
ACS Appl. Mater. Interfaces 2015, 7, 9497−9506

500 ppm of NO, 5 vol % O_2, N_2 balance, and 200 mL/min flow rate. All spectra were recorded by accumulating 100 scans with a resolution of 4 cm^{-1}.

3. RESULTS AND DISCUSSION

3.1. NH_3-SCR Activity. Prior to investigation of the $CeMo_aZr_bO_x$ catalyst, the effect of the Ce:Zr molar ratio on the SCR activity over the $CeZrO_x$ series of catalysts was systematically investigated, and the results are illustrated in Figure S3 in the SI. It was found that the $CeZr_2O_x$ catalyst, with a Ce:Zr molar ratio of 1:2, showed the best NO_x conversion. Therefore, in the later work, the Ce:Zr molar ratio was fixed at 1:2. Figure 1 shows the NO_x conversion and N_2 selectivity as a function of the temperature in the NH_3-SCR reaction over pure MoO_3 and $CeMo_aZr_2O_x$ catalysts under a GHSV of 50000 h^{-1}. $CeZr_2O_x$ exhibited a narrow operation temperature window, and the maximum NO_x conversion was only 90% at 350 °C. However, the addition of a small amount of Mo (Mo:Ce = 0.1:1) to $CeZr_2O_x$ led to an obvious enhancement of the NO_x conversion, implying that the coexistence of Mo and $CeZr_2O_x$ species was very important for promotion of the SCR activity. $CeMo_{0.5}Zr_2O_x$ with a molar ratio of Mo:Ce = 0.5:1 showed the best NH_3-SCR activity and the widest operation temperature window, over which 100% of NO_x conversion was obtained in a wide temperature range (250−400 °C). Further increasing the Mo:Ce molar ratios to 1:1 and 1.5:1 resulted in a decline of the NO_x conversion at both low and high temperatures, which was probably due to the decrease of active Ce sites on the catalyst surface. Similar results were also proposed by Shan et al.[24] and Li et al.[25] when investigating the CeO_2−WO_3 and CeO_2−MoO_3 catalysts. Pure MoO_3 showed negligible activity in the whole temperature range, indicating that the Mo species played the role of only the catalyst promoter rather than the active center for the NH_3-SCR reaction. Although the addition of MoO_3 to the Ce−Zr catalyst could decrease the N_2 selectivity slightly owing to the production of N_2O, the N_2 selectivity over $CeMo_{0.5}Zr_2O_x$ was still more than 80% below 400 °C. The NH_3-SCR results show that some synergistic effects possibly exist between Mo and Ce−Zr species, which will be discussed later in this work.

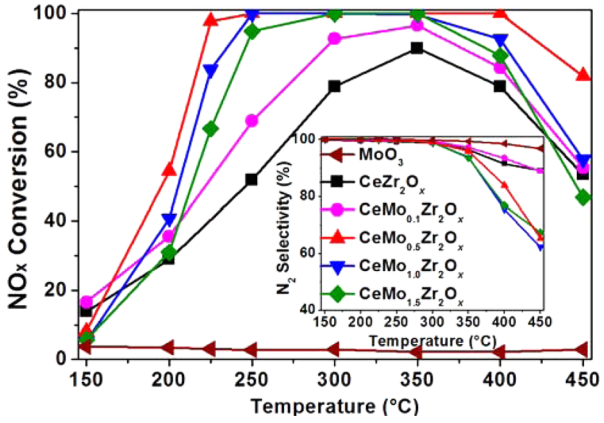

Figure 1. NO_x conversion and N_2 selectivity (inserted) in the NH_3-SCR reaction as a function of the temperature over pure MoO_3 and $CeMo_aZr_2O_x$ (a = 0, 0.1, 0.5, 1.0, 1.5) catalysts. Reaction conditions: [NO] = [NH_3] = 500 ppm, [O_2] = 5 vol %, and GHSV = 50000 h^{-1}.

In addition, the catalytic activity over $CeMo_{0.5}Zr_bO_x$ with various Zr:Ce molar ratios is presented in Figure S4 in the SI. It was obvious that the NO_x conversions over $CeMo_{0.5}Zr_1O_x$ and $CeMo_{0.5}Zr_2O_x$ were similar and higher than those over $CeMo_{0.5}Zr_{0.5}O_x$ and $CeMo_{0.5}Zr_4O_x$ below 300 °C. However, $CeMo_{0.5}Zr_2O_x$ showed better NH_3-SCR activity than $CeMo_{0.5}Zr_1O_x$ above 350 °C. Therefore, in the following studies, $CeMo_{0.5}Zr_2O_x$ was chosen to investigate the "fast SCR" effect and SO_2/H_2O resistance together with the thermal durability of the Mo-containing catalyst.

It was clear that when NO_2 (NO_2:NO = 1:1) was introduced to the reaction gas, the NO_x conversion over $CeMo_{0.5}Zr_2O_x$ at low temperatures was greatly improved because of the "fast SCR" effect and the NO_x conversion was as high as 100% in a wide temperature range from 150 to 400 °C; see Figure S5 in the SI. Therefore, in practical applications, the diesel oxidation catalyst usually is placed in the upstream of the SCR catalyst to convert some NO to NO_2, which has a significant advantage on NO_x removal. To better evaluate the performance of the $CeMo_{0.5}Zr_2O_x$ catalyst, the NH_3-SCR activity over the commercial $V_2O_5(1)$−$WO_3(10)/TiO_2$ catalyst was also conducted and the results are shown in Figure S6 in the SI. NO_x conversion over the $CeMo_{0.5}Zr_2O_x$ catalyst was higher than that over $V_2O_5(1)$−$WO_3(10)/TiO_2$ even though the $CeMo_{0.5}Zr_2O_x$ sample exhibited a relatively low N_2 selectivity at 400 and 450 °C.

3.2. Effect of SO_2 and H_2O. The combustion exhaust often contains some SO_2 and H_2O vapor in the practical application, which may lead to deactivation of the SCR catalyst.[26] Therefore, it is important to investigate the effect of SO_2 and H_2O on the SCR activity. In this work, we studied the effect of 100 ppm of SO_2 and 5 vol % H_2O on the NO_x conversion over $CeMo_{0.5}Zr_2O_x$ at 250 °C under a GHSV of 50000 h^{-1}. As shown in Figure 2A, the introduction of 100 ppm of SO_2 into the reaction atmosphere did not result in any decrease of the NO_x conversion for the first 14 h. With the time increasing, the NO_x conversion showed a slow decrease, which might be associated with the deposition of ammonium sulfate/bisulfate on the surface and blockage of the active sites. However, the conversion was still more than 90% during the measured period. The result in Figure 2B showed that when 5 vol % H_2O was added to the feed stream, the NO_x conversion dramatically decreased from the initial 100% to 40% in the first 2 h and then

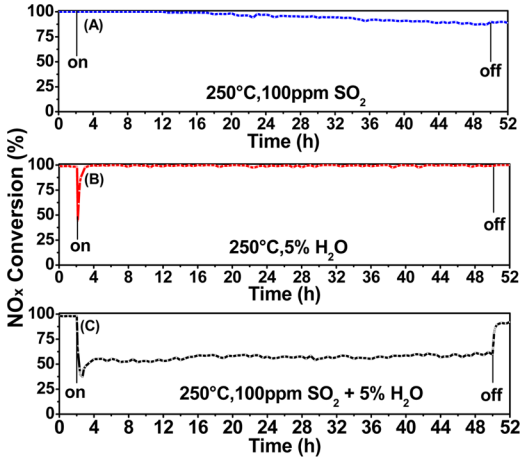

Figure 2. Effect of SO_2 (A), H_2O (B), and SO_2 + H_2O (C) on the SCR activity over the $CeMo_{0.5}Zr_2O_x$ catalyst at 250 °C. Reaction conditions: [NO] = [NH_3] = 500 ppm, [O_2] = 5 vol %, [SO_2] = 100 ppm, [H_2O] = 5 vol %, and GHSV = 50000 h^{-1}.

DOI: 10.1021/acsami.5b00636
ACS Appl. Mater. Interfaces 2015, 7, 9497−9506

recovered to 100%. It was believed that the deactivation effect of H_2O on the activity over catalysts required a long time to achieve steady state. Therefore, when H_2O vapor was first added into the reaction atmosphere, because of the competitive adsorption between H_2O and NH_3/NO over the catalyst, a large amount of H_2O was adsorbed on the active sites where the NH_3/NO adsorbed and activated, leading to a decline of the NO_x conversion. However, when the reaction reached steady state 2 h later, the desorption of excess H_2O adsorbed on the catalyst made it possible for adsorption and activation of NH_3/NO on the active sites, which was responsible for the increase of the NO_x conversion. As presented in Figure 2C, when both 100 ppm of SO_2 and 5 vol % H_2O were introduced, the NO_x conversion also showed a relatively significant decrease to 35% and then maintained nearly 50%; after the SO_2 and H_2O inlets were cut off, the activity was rapidly restored to 90%. In short summary, SO_2 or H_2O alone just showed a negligible influence on the SCR activity; the coexistence of SO_2 and H_2O decreased the conversion significantly, indicating that some synergistic inhibition effect between SO_2 and H_2O was present on the SCR activity; however, the effect was reversible to a certain extent. It was believed that when both SO_2 and H_2O were introduced to the reaction atmosphere, the deactivation effect might be not only related to the competitive adsorption between H_2O and NH_3/NO_x but also associated with the formation of ammonium sulfate together with high thermally stable $Ce(SO_4)_2$/$Ce_2(SO_4)_3$ on the active sites because of SO_2, which suggested that both H_2O and SO_2 could inhibit the adsorption and activation of NH_3/NO_x on the active sites, leading to an obvious decline of the NO_x conversion.

The reaction temperature had a great impact on the performance of the SCR catalyst. Therefore, the SO_2/H_2O resistance of the $CeMo_{0.5}Zr_2O_x$ catalyst was also conducted at 400 °C. As shown in Figure S7A in the SI, the NO_x conversion still remained 100% after the introduction of 100 ppm of SO_2 at 400 °C for 48 h, which was higher than that at 250 °C in Figure 2A. The results indicated that the SO_2 tolerance was improved as the reaction temperature increased from 250 to 400 °C. As presented in Figure S7B in the SI, 5% H_2O alone has an insignificant effect on the SCR activity over the $CeMo_{0.5}Zr_2O_x$ catalyst at 400 °C and NO_x conversion was almost 100%. The results in Figure S7C in the SI demonstrated that when both SO_2 and H_2O were introduced to the reaction gas, the NO_x conversion exhibited a trend similar to that in Figure 2C.

In addition, as shown in Figure S8 in the SI, 500 ppm of SO_2 was added to the reaction gas at 250 °C to evaluate the SO_2 resistance of the $CeMo_{0.5}Zr_2O_x$ catalyst. The results showed that the NO_x conversion was greatly declined from the initial 100% to 30%, which was greatly different from the effect of 100 ppm on the NO_x conversion in Figure 2B, indicating that a higher concentration of SO_2 would lead to a serious deactivation of the catalyst. However, in real applications, the concentration of SO_2 from diesel engine exhaust depends on the sulfur content of the diesel fuel. In recent years, SO_2 in diesel engine exhaust is only tens of parts per million, which is much lower than 500 ppm.

In order to further investigate the influence of SO_2/H_2O treatment on the $CeMo_{0.5}Zr_2O_x$ catalyst, the NH_3-SCR activity as a function of the reaction temperature of $CeMo_{0.5}Zr_2O_x$ catalysts treated in SO_2/H_2O for 48 h in Figure 2 was retested, and the results are shown in Figure 3. Prior to the activity measurements of $CeMo_{0.5}Zr_2O_x$ catalysts treated in SO_2/H_2O

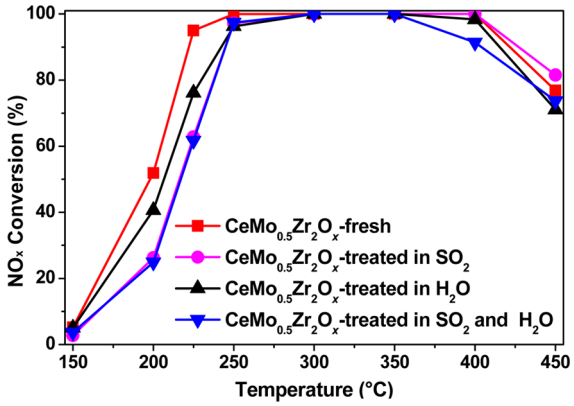

Figure 3. NO_x conversion in the NH_3-SCR reaction as a function of the temperature over $CeMo_{0.5}Zr_2O_x$ catalysts after treatment in SO_2/H_2O for 48 h. Reaction conditions: [NO] = [NH_3] = 500 ppm, [O_2] = 5 vol %, and GHSV = 50000 h^{-1}.

for 48 h, the catalysts were calcined at 400 °C for 1 h to eliminate the ammonium sulfate deposited on the surface of the catalysts. Compared to the fresh $CeMo_{0.5}Zr_2O_x$ catalyst, the SCR activity of the catalysts treated in SO_2/H_2O showed a slight decrease between 150 and 250 °C. However, the NO_x conversion was still kept at more than 90% in the temperature range from 250 to 400 °C. Therefore, the $CeMo_{0.5}Zr_2O_x$ catalyst exhibits strong resistance to SO_2 and H_2O poisoning, which can be used to remove NO_x from diesel engine exhaust containing a certain amount of SO_2 and H_2O vapor.

3.3. Effect of GHSV. The NO_x conversion over $CeMo_{0.5}Zr_2O_x$ under different GHSVs is shown in Figure 4.

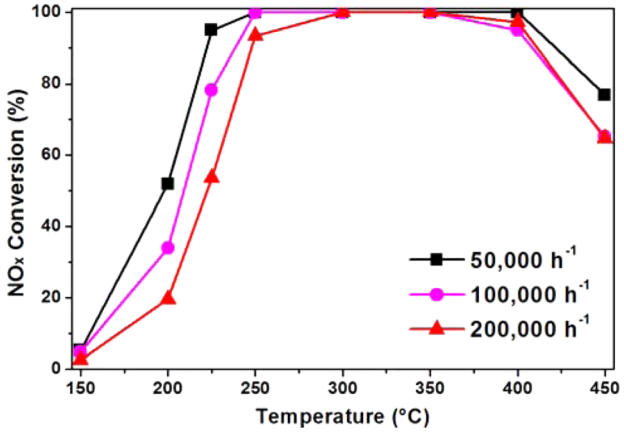

Figure 4. NO_x conversion in the NH_3-SCR reaction as a function of the temperature over the $CeMo_{0.5}Zr_2O_x$ catalyst under different GHSVs. Reaction conditions: [NO] = [NH_3] = 500 ppm and [O_2] = 5 vol %.

It can be seen that NO_x conversion below 250 °C decreased slightly when GHSV was increased from 50000 to 200000 h^{-1}. However, even at the highest GHSV of 200000 h^{-1}, NO_x conversion was still more than 90% in the temperature range from 250 to 400 °C. The effect of GHSV on the NO_x conversion at high temperature was weaker than that at low temperature. These results indicated that the $CeMo_{0.5}Zr_2O_x$ catalyst is highly effective for the removal of NO_x in a wide temperature range from 250 to 400 °C even when the reaction condition is harsh.

DOI: 10.1021/acsami.5b00636
ACS Appl. Mater. Interfaces 2015, 7, 9497−9506

3.4. Thermal Stability Test. In practical use, the NH_3-SCR catalyst should also have good thermal stability in the long-term deNO$_x$ process. At the same time, to meet tougher emission standards of diesel engine exhaust, the diesel particulate filter (DPF) has to be used. The diesel exhaust gas temperature can reach above 700 °C during the regeneration process of the DPF system.[27] Therefore, the $CeMo_{0.5}Zr_2O_x$ catalysts were calcined at different temperatures (500, 550, 600, 650, 700, and 750 °C) for 8 h to test the thermal stability, and the results are illustrated in Figure 5A. As the calcination temperature

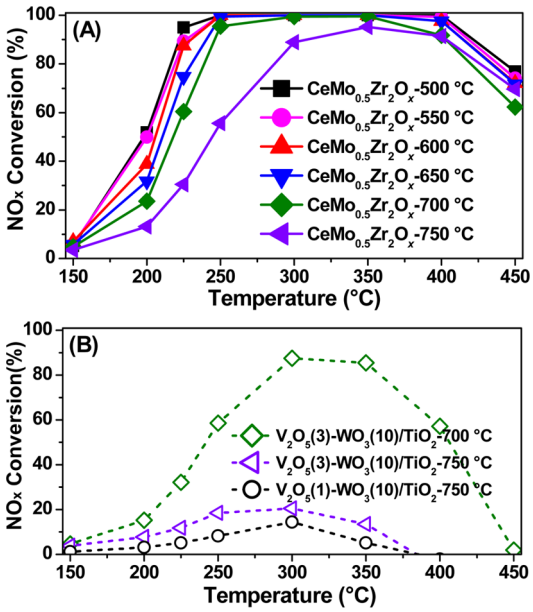

Figure 5. NO_x conversion in the NH_3-SCR reaction as a function of the temperature over $CeMo_{0.5}Zr_2O_x$ (A) and V_2O_5–WO_3/TiO_2 (B) catalysts calcined at different temperatures for 8 h. Reaction conditions: [NO] = [NH_3] = 500 ppm, [O_2] = 5 vol %, and GHSV = 50000 h^{-1}.

increased from 500 to 700 °C, the NO_x conversion below 250 °C showed a slight and monotonic decrease, while the conversion above 250 °C was quite similar. Further increasing the calcination temperature to 750 °C resulted in an obvious decrease of the NH_3-SCR activity at both low and high temperatures, which might be caused by the decrease of the surface area and sintering of the active component. For comparison purposes, the SCR activity of commercial V_2O_5–WO_3/TiO_2 catalysts with various V_2O_5 contents calcined at 700 or 750 °C was also studied. As shown in Figure 5B, these catalysts show poor activity in the whole temperature range, which might be due to the decrease of the surface area, the anatase-to-rutile transition of TiO_2, and the loss of vanadia.[15] Compared to the commercial V_2O_5–WO_3/TiO_2 catalyst, the $CeMo_{0.5}Zr_2O_x$ catalyst exhibits much better high-temperature stability.

Moreover, as shown in Figure S9 in the SI, the $CeMo_{0.5}Zr_2O_x$ catalyst hydrothermally treated at 700 °C for 48 h still exhibited high NH_3-SCR activity, over which more than 80% NO_x conversion was obtained between 300 and 400 °C. Further increasing the aging temperature to 760 °C would resulted in an obvious diminution of the SCR activity, indicating that $CeMo_{0.5}Zr_2O_x$ could only be used below 700 °C. The hydrothermal stability of the $CeMo_{0.5}Zr_2O_x$ catalyst needs to be improved further in future studies.

3.5. N_2 Physisorption and XRD Results. The specific surface area and BJH desorption pore volume of MoO_3, $CeMo_aZr_2O_x$, and $CeMo_{0.5}Zr_2O_x$ calcined at different temperatures are shown in Tables 1 and 2, respectively. As shown in

Table 1. BET Surface Area, Pore Volume, and CeO_2 Crystallite Size of MoO_3 and $CeMo_aZr_2O_x$

catalyst	S_{BET}[a] (m^2/g)	pore volume[b] (cm^3/g)	CeO_2 crystallite size[c] (nm)
MoO_3	1.4	0.006	
$CeZr_2O_x$	107.3	0.097	11.8
$CeMo_{0.1}Zr_2O_x$	109.1	0.079	11.4
$CeMo_{0.5}Zr_2O_x$	82.6	0.037	11.2
$CeMo_{1.0}Zr_2O_x$	61.0	0.028	9.6
$CeMo_{1.5}Zr_2O_x$	51.5	0.027	9.5

[a]BET surface area. [b]BJH desorption pore volume. [c]CeO_2 crystallite size calculated by the Scherrer equation from the XRD results.

Table 2. BET Surface Area, Pore Volume, and CeO_2 Crystallite Size of $CeMo_{0.5}Zr_2O_x$ Calcined at Different Temperatures for 8 h

catalyst	S_{BET} (m^2/g)	pore volume (cm^3/g)	CeO_2 crystallite size (nm)
$CeMo_{0.5}Zr_2O_x$-500 °C	77.8	0.038	12.1
$CeMo_{0.5}Zr_2O_x$-550 °C	75.8	0.040	12.1
$CeMo_{0.5}Zr_2O_x$-600 °C	71.3	0.058	14.8
$CeMo_{0.5}Zr_2O_x$-650 °C	47.7	0.070	15.9
$CeMo_{0.5}Zr_2O_x$-700 °C	33.0	0.070	21.2
$CeMo_{0.5}Zr_2O_x$-750 °C	21.1	0.063	22.4

Table 1, the addition of a small amount of Mo (Mo:Ce = 0.1:1) to $CeZr_2O_x$ showed a negligible effect on the surface area. However, when the molar ratio of Mo:Ce was more than 0.5:1, the surface area of the catalysts decreased obviously as the Mo loading increased because of the quite small surface area of MoO_3. It was also reported that the addition of Mo could reduce the surface area of MoO_3–CeO_2 catalysts, which were prepared by coprecipitation using urea as the precipitant.[28] Meanwhile, the doping of Mo into $CeZr_2O_x$ decreased the pore volume.

Table 2 shows the surface area and pore volume of $CeMo_{0.5}Zr_2O_x$ calcined at different temperatures. It could be seen that increasing the calcination temperature from 500 to 750 °C resulted in a decrease of the surface area from 77.8 to 21.1 m^2/g, while the pore volume increased gradually. The decrease of the surface area and the sintering of the active component at high calcination temperatures might be responsible for the decrease of the NO_x conversion at low temperatures.[29]

The XRD results of the catalysts with different Mo loadings are summarized in Figure 6A. The reflections provided typical diffraction patterns for the CeO_2 cubic phase (JCPDS 34-0394) and the ZrO_2 tetragonal phase (JCPDS 50-1089). No diffraction peaks attributed to Mo species were detected in the XRD patterns, implying that Mo species were finely dispersed on the surface of the catalysts or existed as amorphous species. Furthermore, as shown in Table 1, the

DOI: 10.1021/acsami.5b00636
ACS Appl. Mater. Interfaces 2015, 7, 9497–9506

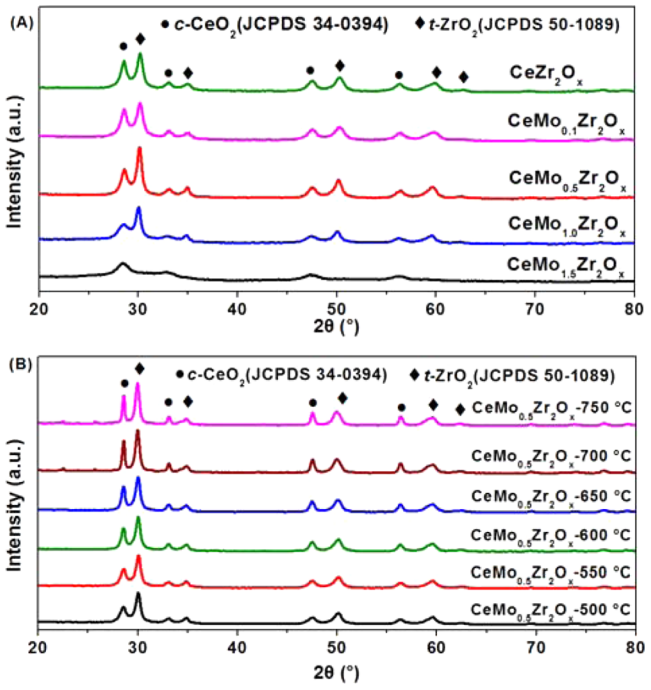

Figure 6. Powder XRD of $CeMo_aZr_2O_x$ catalysts with different Mo loadings (A) and $CeMo_{0.5}Zr_2O_x$ catalysts calcined at different temperatures for 8 h (B).

average crystallite size of CeO_2 calculated by the Scherrer equation decreased slightly as the Mo content increased. As presented in Figure 6B, the XRD patterns of $CeMo_{0.5}Zr_2O_x$ samples calcined at various temperatures from 500 to 750 °C for 8 h showed typical diffraction peaks for the cubic CeO_2 and tetragonal ZrO_2 phases, and no diffraction peaks for Mo species were detected. With increasing calcination temperature, the intensities of all of the diffraction peaks increased slightly and the CeO_2 average crystallite size increased from 12.1 to 22.4 nm (Table 2). However, after high-temperature calcination, the positions of the diffraction peaks stayed the same, indicating that changes of the crystallite phases of CeO_2 and ZrO_2 did not occur in this process.

3.6. Raman Spectra. Visible Raman spectra were also applied to characterize the $CeMo_aZr_2O_x$ catalysts, and the results are presented in Figure 7. $CeZr_2O_x$ showed an obvious band at 463 cm^{-1} and three weak peaks at about 630, 315, and

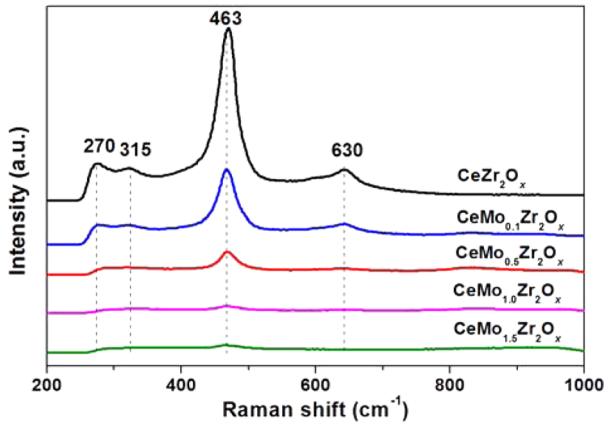

Figure 7. Visible Raman spectra of the $CeMo_aZr_2O_x$ catalysts.

270 cm^{-1}. The band at 463 cm^{-1} was due to the Raman-active F_{2g} mode of the CeO_2 fluorite structure.[30] The band at 630 cm^{-1} could be a consequence of the lattice contraction brought about by Zr ion insertion.[9] The bands at 315 and 270 cm^{-1} could be assigned to the Zr phase (t-ZrO_2).[31−33] With an increase of the Mo content, the Raman spectral intensity of CeO_2 decreased significantly, which proved that the introduction of Mo inhibited growth of the CeO_2 particle size.[25] These analytical results are in good accordance with the conclusion drawn from XRD results. In combination with the XRD and Raman results, it could be concluded that Mo species were mainly present in a highly dispersed state and the addition of Mo resulted in a decrease of the CeO_2 crystallite size. However, the CeO_2 crystallite size was not the only factor leading to the discrepancy of the catalytic activity between different catalysts.

3.7. H_2-TPR. H_2-TPR experiments were conducted to investigate the redox ability of the catalysts, and the results are shown in Figure 8. For the $CeZr_2O_x$ catalyst, the reduction

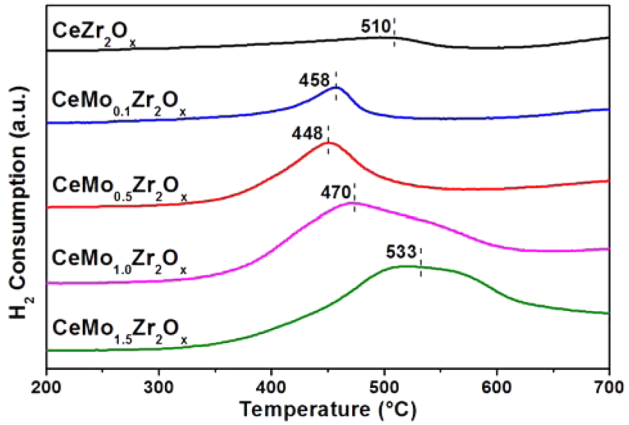

Figure 8. H_2-TPR profiles of the $CeMo_aZr_2O_x$ catalysts.

peak at about 510 °C was attributed to the reduction of surface Ce^{4+} to Ce^{3+}.[25,34] After the introduction of Mo to $CeZr_2O_x$, the reduction peak of surface Ce^{4+} moved to lower temperatures, which indicated that the mobility of surface O was greatly improved because of the strong synergetic effect among Zr, Ce, and Mo species. It is believed that the synergetic effect gave rise to severe structural distortion and abundant O defects.[16,35] The O defects facilitated O diffusion from the subsurface layers and might progressively proceed deeper into the bulk.[36,37] All of the above features were beneficial for the SCR activity. In addition, it was also reported that the mobility of surface O on the $CeMoAlO_x$ catalyst was enhanced by Mo addition.[38] $CeMo_{0.5}Zr_2O_x$ exhibited the lowest reduction temperature at 448 °C, which was in harmony with its highest SCR activity. However, upon a further increase of the Mo/Ce molar ratios from 0.5 to 1.5, the reduction peaks attributed to the overlap of Ce and Mo species shifted to higher temperatures, which might be caused by the coverage of Mo species. These results indicate that the stronger oxidation reduction ability of $CeMo_{0.5}Zr_2O_x$ benefits the excellent SCR reaction performance.

3.8. In Situ DRIFTS Studies. *3.8.1. NH_3 Adsorption.* In situ DRIFTS spectra of NH_3 adsorption at 200 °C were measured to examine the change of acidity on the catalysts after Mo addition, and the results are shown in Figure 9A. After exposure to NH_3, the catalysts were covered by several kinds of NH_3 species. The bands at 1668 cm^{-1} and 1425, 1440, and 1414 cm^{-1} were assigned to symmetric and asymmetric bending

DOI: 10.1021/acsami.5b00636
ACS Appl. Mater. Interfaces 2015, 7, 9497−9506

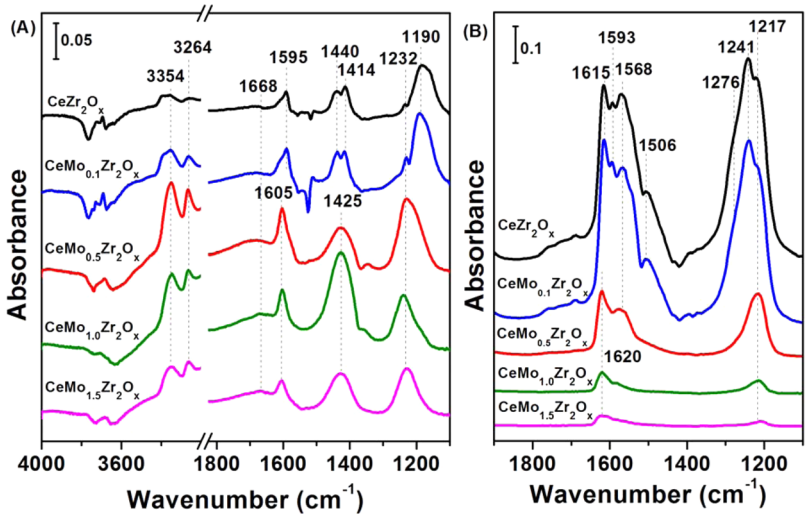

Figure 9. In situ DRIFTS of NH_3 adsorption (A) and NO + O_2 adsorption (B) at 200 °C on the $CeMo_aZr_2O_x$ series of catalysts.

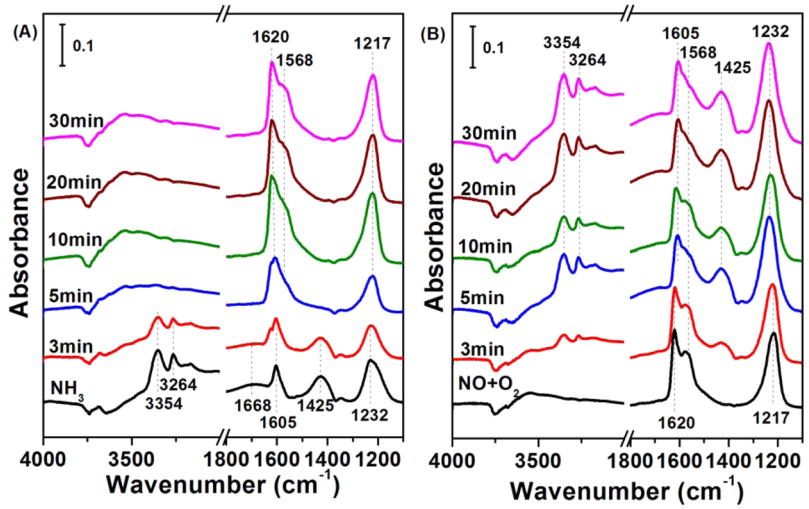

Figure 10. In situ DRIFTS of NO + O_2 reacted with preadsorbed NH_3 species (A) and NH_3 reacted with preadsorbed NO_x species (B) at 200 °C on the $CeMo_{0.5}Zr_2O_x$ catalyst.

vibrations, respectively, of NH_4^+ species on Brønsted acid sites.[5,22,39−41] The bands at 1605 and 1595 cm^{-1} and at 1232 and 1190 cm^{-1} were attributed to asymmetric and symmetric bending vibrations, respectively, of the N−H bonds in coordinated NH_3 linked to Lewis acid sites, respectively.[42,43] The bands at 3354 and 3264 cm^{-1} ascribed to N−H stretching modes of coordinated NH_3 were also observed.[23] Some negative bands around 3700 cm^{-1} were also found that could be assigned to hydroxyl consumption due to interaction between the hydroxyl groups and NH_3 to form NH_4^+.[5,35]

Compared to $CeZr_2O_x$, the addition of Mo enhanced the band intensities of adsorbed NH_4^+ greatly. This meant that the introduction of Mo resulted in more Brønsted acid sites on the catalyst surface, and similar results were also found on CeO_2−MoO_3 catalysts in the published literature.[25,28] For coordinated NH_3 bound to Lewis acid sites, the band intensity first had an obvious increase and then showed a decrease when the molar ratio of Mo:Ce was higher than 0.5:1. In addition, the NH_3-TPD results indicated that the total amount of NH_3 adsorbed on $CeMo_{0.5}Zr_2O_x$ was higher than that on the $CeZr_2O_x$ catalyst; see Figure S10A in the SI. The band intensity due to Lewis acid sites over $CeMo_{0.5}Zr_2O_x$ was the highest among the series of catalysts, which was in good accordance with the results of the SCR activity. Although the intensity of adsorbed NH_4^+ over $CeMo_{1.0}Zr_2O_x$ was stronger than that over $CeMo_{0.5}Zr_2O_x$, $CeMo_{0.5}Zr_2O_x$ exhibited higher band intensity attributed to coordinated NH_3 adsorption. It can be concluded that the Lewis acid sites over the $CeMo_{0.5}Zr_2O_x$ catalyst are responsible for its highest SCR activity. Peng et al. investigated the structure activity relationship of the MoO_3−CeO_2 catalyst for NH_3-SCR of NO_x and found that the Lewis acid sites could be involved in the reaction even more rapidly than the Brønsted acid sites.[28]

3.8.2. NO + O_2 Adsorption. Figure 9B presents the in situ DRIFTS results of NO_x adsorption at 200 °C. After NO + O_2 adsorption and N_2 purge, several distinct bands attributed to monodentate nitrate (1506 and 1276 cm^{-1}), bidentate nitrate (1593 and 1568 cm^{-1}), and bridging nitrate (1615, 1620, 1241, and 1217 cm^{-1}) appeared.[39,44−46] With increasing Mo addition content, the bands due to adsorbed nitrate species showed an obvious decrease in intensity, and only bridging nitrate species were observed on the $CeMo_{1.5}Zr_2O_x$ catalyst. It is concluded that the addition of Mo significantly limits the adsorption of nitrate species, which could also be confirmed by the results

DOI: 10.1021/acsami.5b00636
ACS Appl. Mater. Interfaces 2015, 7, 9497−9506

drawn from NO-TPD in Figure S10B in the SI. It is believed that the introduction of MoO_3 resulted in the formation of more acid sites accompanied by the reduction of basic sites where nitrate adsorbed.[22] The inhibitory effect of Mo on the adsorption of nitrate species has also been reported by other researchers on the MoO_3−CeO_2/TiO_2[22] and $CeMo_{0.5}AlO_x$[38] catalysts for the NH_3-SCR process.

3.8.3. Reaction between NO + O_2 and Adsorbed NH_3 Species. To investigate the reactivity of adsorbed NH_3 species in the SCR reaction on the $CeMo_{0.5}Zr_2O_x$ catalyst, in situ DRIFTS of the reaction between preadsorbed NH_3 and NO + O_2 at 200 °C was recorded as a function of time (Figure 10A). After the introduction of NO + O_2, the bands ascribed to ionic NH_4^+ (1668 and 1425 cm^{-1}) and coordinated NH_3 (3354, 3264, 1605, and 1232 cm^{-1}) showed an apparent decrease in intensity, and all of the bands were replaced by nitrate species after 5 min. This indicates that both coordinated NH_3 and ionic NH_4^+ on the $CeMo_{0.5}Zr_2O_x$ catalyst could react as reducing agents to reduce NO_x. Although coordinated NH_3 over the $CeMo_{0.5}Zr_2O_x$ catalyst was responsible for its highest SCR activity, ionic NH_4^+ could also be involved in the SCR reaction. It could be concluded that the addition of Mo to $CeZr_2O_x$ resulted in more coordinated NH_3 and ionic NH_4^+, both of which could participate in the NH_3-SCR reaction.

3.8.4. Reaction between NH_3 and Adsorbed NO_x Species. The reactivity of absorbed NO_x species in the SCR reaction on the $CeMo_{0.5}Zr_2O_x$ catalyst was also investigated by the in situ DRIFTS of the reaction between preadsorbed NO_x and NH_3 at 200 °C, and the results are shown in Figure 10B. After exposure to NO + O_2, the catalyst was mainly covered by bidentate nitrate (1568 cm^{-1}) and bridging nitrate (1620 and 1217 cm^{-1}). When NH_3 was introduced, the bridging nitrate was greatly decreased and disappeared in 5 min, while the bidentate nitrate did not show an obvious decrease. At the same time, the bands attributed to ionic NH_4^+ (1668 and 1425 cm^{-1}) and coordinated NH_3 (3354, 3264, 1605, and 1232 cm^{-1}) were observed after 5 min. The results indicate that bridging nitrate rather than bidentate nitrate can react with NH_3. Although the addition of Mo inhibited the adsorption of nitrate species on the surface, the reaction between adsorbed nitrate species and NH_3 still played a significant role in the reduction of NO_x. Judging from Figure 9B, the amount of nitrate species on $CeMo_{0.1}Zr_2O_x$ was higher than that on other Mo-containing catalysts, indicating that $CeMo_{0.1}Zr_2O_x$ should be an excellent catalyst for the SCR reaction. However, the lack of enough NH_3 species on the surface of $CeMo_{0.1}Zr_2O_x$ (Figure 9A) lowered SCR conversion, as seen in Figure 1. The adsorption amounts of coordinated NH_3 and nitrate species on $CeMo_{0.5}Zr_2O_x$ were both higher than that on $CeMo_{1.0}Zr_2O_x$ or $CeMo_{1.5}Zr_2O_x$. It is believed that the adsorption of NH_3 and NO_x was considered to be essential in the NH_3-SCR reaction at low temperatures. Liu et al. investigated the promoting effect of MoO_3 on the NH_3-SCR activity over the CeO_2/TiO_2 catalyst and believed that the unsaturated Mo resulted in more acid sites, which was favorable for the adsorption of NH_3, thus improving the low-temperature activity.[22] Nitro and nitrate groups were beneficial to promote the SCR process at low temperatures over an F-doped CeO_2−TiO_2 catalyst.[47] In addition, the results in Figure 10 show that both adsorbed NH_3 species (coordinated NH_3, ionic NH_4^+) and adsorbed bridging nitrate species were active in the NH_3-SCR action. Therefore, it was reasonable to conclude that the high adsorption amounts of NH_3 and nitrate species were favorable for the high activity of the $CeMo_{0.5}Zr_2O_x$ catalyst.

4. CONCLUSIONS

A novel Mo-promoted Ce−Zr catalyst prepared by a homogeneous precipitation method was used for NH_3-SCR of NO_x. The $CeMo_{0.5}Zr_2O_x$ catalyst with a Mo:Ce molar ratio of 0.5:1 showed high SCR activity, SO_2/H_2O durability, and thermal stability under test conditions. Characterization results indicated that Mo addition inhibited growth of the CeO_2 particle size, improved the redox ability, and increased the amount of surface acidity, especially the Lewis acidity. Coordinated NH_3 and ionic NH_4^+ species together with bridging nitrate were active over the $CeMo_{0.5}Zr_2O_x$ catalyst during the NH_3-SCR reaction. All of the features above are responsible for the excellent NH_3-SCR performance.

■ ASSOCIATED CONTENT

Supporting Information

pH value variation during the preparation, distribution of Zr, Ce, and Mo on $CeMo_{0.5}Zr_2O_x$ catalyst, designed and actual bulk molar ratios, NO_x conversion and N_2 selectivity in NH_3-SCR reaction over V_2O_5-WO_3/TiO_2, effect of SO_2, H_2O, SO_2 + H_2O at 400 °C, and 500 ppm SO_2 at 250 °C on the SCR activity, and NH_3-TPD and NO-TPD results. The Supporting Information is available free of charge on the ACS Publications website at DOI: 10.1021/acsami.5b00636.

■ AUTHOR INFORMATION

Corresponding Authors

*E-mail: fudongliu@lbl.gov or lfd1982@gmail.com. Tel: +86 10 62849123. Fax: +86 10 62849123.

*E-mail: honghe@rcees.ac.cn. Tel: +86 10 62849123. Fax: +86 10 62849123.

Present Address

†F.L.: Materials Sciences Division, Lawrence Berkeley National Laboratory, 1 Cyclotron Road, Berkeley, CA 94720.

Author Contributions

The manuscript was written through contributions of all authors. All authors have given approval to the final version of the manuscript.

Notes

The authors declare no competing financial interest.

■ ACKNOWLEDGMENTS

This work was supported by the National Natural Science Foundation of China (Grant 51221892) and the Ministry of Science and Technology China (Grant 2013AA065301).

■ REFERENCES

(1) Pavulescu, V. I.; Grange, P.; Delmon, B. Catalytic Removal of NO. *Catal. Today* **1998**, *46*, 233−316.

(2) Koebel, M.; Elsener, M.; Kleemann, M. Urea-SCR: a Promising Technique to Reduce NO_x Emissions from Automotive Diesel Engines. *Catal. Today* **2000**, *59*, 335−345.

(3) Brandenberger, S.; Kröcher, O.; Tissler, A.; Althoff, R. The State of the Art in Selective Catalytic Reduction of NO_x by Ammonia Using Metal-Exchanged Zeolite Catalysts. *Catal. Rev.* **2008**, *50*, 492−531.

(4) Grossale, A.; Nova, I.; Tronconi, E. Ammonia Blocking of the "Fast SCR" Reactivity over a Commercial Fe-zeolite Catalyst for Diesel Exhaust Aftertreatment. *J. Catal.* **2009**, *265*, 141−147.

(5) Liu, F. D.; He, H.; Ding, Y.; Zhang, C. B. Effect of Manganese Substitution on the Structure and Activity of Iron Titanate Catalyst for

DOI: 10.1021/acsami.5b00636
ACS Appl. Mater. Interfaces 2015, 7, 9497−9506

the Selective Catalytic Reduction of NO with NH_3. *Appl. Catal., B* **2009**, *93*, 194−204.
(6) Paier, J.; Penschke, C.; Sauer, J. Oxygen Defects and Surface Chemistry of Ceria: Quantum Chemical Studies Compared to Experiment. *Chem. Rev.* **2013**, *113*, 3949−3985.
(7) Ma, Z. R.; Weng, D.; Wu, X. D.; Si, Z. C. Effects of WO_x Modification on the Activity, Adsorption and Redox Properties of CeO_2 Catalyst for NO_x Reduction with Ammonia. *J. Environ. Sci. (Beijing, China)* **2012**, *24*, 1305−1316.
(8) Zhang, D.; Du, X.; Shi, L.; Gao, R. Shape-Controlled Synthesis and Catalytic Application of Ceria Nanomaterials. *Dalton Trans.* **2012**, *41*, 14455−75.
(9) Shang, D. H.; Cai, W.; Zhao, W.; Bu, Y. F.; Zhong, Q. Catalytic Oxidation of NO to NO_2 over Co−Ce−Zr Solid Solutions: Enhanced Performance of Ce−Zr Solid Solution by Co. *Catal. Lett.* **2014**, *144*, 538−544.
(10) Hori, C. E.; Permana, H.; Ng, K. Y. S.; Brenner, A.; More, K.; Rahmoeller, K. M.; Belton, D. Thermal Stability of Oxygen Storage Properties in a Mixed CeO_2−ZrO_2 System. *Appl. Catal., B* **1998**, *16*, 105−117.
(11) Terribile, D.; Trovarelli, A.; Llorca, J.; de Leitenburg, C.; Dolcetti, G. The Preparation of High Surface Area CeO_2−ZrO_2 Mixed Oxides by a Surfactant-Assisted Approach. *Catal. Today* **1998**, *43*, 79−88.
(12) Si, Z.; Weng, D.; Wu, X.; Yang, J.; Wang, B. Modifications of CeO_2−ZrO_2 Solid Solutions by Nickel and Sulfate as Catalysts for NO Reduction with Ammonia in Excess O_2. *Catal. Commun.* **2010**, *11*, 1045−1048.
(13) Maitarad, P.; Han, J.; Zhang, D.; Shi, L.; Namuangruk, S.; Rungrotmongkol, T. Structure−Activity Relationships of NiO on CeO_2 Nanorods for the Selective Catalytic Reduction of NO with NH_3: Experimental and DFT Studies. *J. Phys. Chem. C* **2014**, *118*, 9612−9620.
(14) Shen, B.; Wang, Y.; Wang, F.; Liu, T. The Effect of Ce−Zr on NH_3-SCR Activity over $MnO_x(0.6)/Ce_{0.5}Zr_{0.5}O_2$ at Low Temperature. *Chem. Eng. J.* **2014**, *236*, 171−180.
(15) Li, Y.; Cheng, H.; Li, D.; Qin, Y.; Xie, Y.; Wang, S. WO_3/CeO_2−ZrO_2, a Promising Catalyst for Selective Catalytic Reduction (SCR) of NO_x with NH_3 in Diesel Exhaust. *Chem. Commun.* **2008**, 1470−1472.
(16) Cai, S.; Zhang, D.; Zhang, L.; Huang, L.; Li, H.; Gao, R.; Shi, L.; Zhang, J. Comparative study of 3D ordered macroporous $Ce_{0.75}Zr_{0.2}M_{0.05}O_{2-\delta}$ (M = Fe, Cu, Mn, Co) for selective catalytic reduction of NO with NH_3. *Catal. Sci. Technol.* **2014**, *4*, 93−101.
(17) Gao, R. H.; Zhang, D. S.; Maitarad, P.; Shi, L. Y.; Rungrotmongkol, T.; Li, H. R.; Zhang, J. P.; Cao, W. G. Morphology-Dependent Properties of MnO_x/ZrO_2−CeO_2 Nanostructures for the Selective Catalytic Reduction of NO with NH_3. *J. Phys. Chem. C* **2013**, *117*, 10502−10511.
(18) Si, Z. C.; Weng, D.; Wu, X. D.; Ran, R.; Ma, Z. R. NH_3-SCR Activity, Hydrothermal Stability, Sulfur Resistance and Regeneration of $Ce_{0.75}Zr_{0.25}O_2$−PO_4^{3-} Catalyst. *Catal. Commun.* **2012**, *17*, 146−149.
(19) Busca, G.; Lietti, L.; Ramis, G.; Berti, F. Chemical and Mechanistic Aspects of the Selective Catalytic Reduction of NO_x by Ammonia over Oxide Catalysts: A Review. *Appl. Catal., B* **1998**, *18*, 1−36.
(20) Lietti, L.; Nova, I.; Forzatti, P. Selective Catalytic Reduction (SCR) of NO by NH_3 over TiO_2-supported V_2O_5−WO_3 and V_2O_5−MoO_3 Catalysts. *Top. Catal* **2000**, *11*, 111−122.
(21) Maqbool, M. S.; Pullur, A. K.; Ha, H. P. Novel Sulfation Effect on Low-Temperature Activity Enhancement of CeO_2-Added Sb−V_2O_5/TiO_2 Catalyst for NH_3-SCR. *Appl. Catal., B* **2014**, *152*, 28−37.
(22) Liu, Z. M.; Zhang, S. X.; Li, J. H.; Ma, L. L. Promoting Effect of MoO_3 on the NO_x Reduction by NH_3 over CeO_2/TiO_2 Catalyst Studied with in situ DRIFTS. *Appl. Catal., B* **2014**, *144*, 90−95.
(23) Shan, W. P.; Liu, F. D.; He, H.; Shi, X. Y.; Zhang, C. B. A superior Ce−W−Ti Mixed Oxide Catalyst for the Selective Catalytic Reduction of NO_x with NH_3. *Appl. Catal., B* **2012**, *115*, 100−106.
(24) Shan, W.; Liu, F.; He, H.; Shi, X.; Zhang, C. Novel Cerium−Tungsten Mixed Oxide Catalyst for the Selective Catalytic Reduction of NO_x with NH_3. *Chem. Commun.* **2011**, *47*, 8046−8048.
(25) Li, X.; Li, Y. Selective Catalytic Reduction of NO with NH_3 over Ce−Mo−O_x Catalyst. *Catal. Lett.* **2013**, *144*, 165−171.
(26) Lee, K. J.; Kumar, P. A.; Maqbool, M. S.; Rao, K. N.; Song, K. H.; Ha, H. P. Ceria Added Sb−V_2O_5/TiO_2 Catalysts for Low Temperature NH_3-SCR: Physico-Chemical Properties and Catalytic Activity. *Appl. Catal., B* **2013**, *142*, 705−717.
(27) Wang, X. Q.; Shi, A. J.; Duan, Y. F.; Wang, J.; Shen, M. Q. Catalytic Performance and Hydrothermal Durability of CeO_2−V_2O_5−ZrO_2/WO_3−TiO_2 Based NH_3-SCR Catalysts. *Catal. Sci. Technol.* **2012**, *2*, 1386−1395.
(28) Peng, Y.; Qu, R.; Zhang, X.; Li, J. The Relationship between Structure and Activity of MoO_3−CeO_2 Catalysts for NO Removal: Influences of Acidity and Reducibility. *Chem. Commun.* **2013**, *49*, 6215−6217.
(29) Liu, F. D.; He, H.; Lian, Z. H.; Shan, W. P.; Xie, L. J.; Asakura, K.; Yang, W. W.; Deng, H. Highly Dispersed Iron Vanadate Catalyst Supported on TiO_2 for the Selective Catalytic Reduction of NO_x with NH_3. *J. Catal.* **2013**, *307*, 340−351.
(30) Reddy, B. M.; Lakshmanan, P.; Khan, A. Investigation of Surface Structures of Dispersed V_2O_5 on CeO_2−SiO_2, CeO_2−TiO_2, and CeO_2−ZrO_2 Mixed Oxides by XRD, Raman, and XPS Techniques. *J. Phys. Chem. B* **2004**, *108*, 16855−16863.
(31) Gao, S.; Chen, X.; Wang, H.; Mo, J.; Wu, Z.; Liu, Y.; Weng, X. Ceria Supported on Sulfated Zirconia as a Superacid Catalyst for Selective Catalytic Reduction of NO with NH_3. *J. Collid Interface Sci.* **2013**, *394*, 515−521.
(32) Letichevsky, S.; Tellez, C. A.; Avillez, R. R. d.; Silva, M. I. P. d.; Fraga, M. A.; Appel, L. G. Obtaining CeO_2−ZrO_2 mixed oxides by coprecipitation: role of preparation conditions. *Appl. Catal., B* **2005**, *58*, 203−210.
(33) Si, R. Urea-Based Hydrothermally Derived Homogeneous Nanostructured $Ce_{1-x}Zr_xO_2$ (x = 0−0.8) Solid Solutions: A Strong Correlation between Oxygen Storage Capacity and Lattice Strain. *J. Phys. Chem. B* **2004**, *108*, 12481−12488.
(34) Peng, Y.; Li, J.; Chen, L.; Chen, J.; Han, J.; Zhang, H.; Han, W. Alkali Metal Poisoning of a CeO_2−WO_3 Catalyst used in the Selective Catalytic Reduction of NO_x with NH_3: An Experimental and Theoretical Study. *Environ. Sci. Technol.* **2012**, *46*, 2864−2869.
(35) Xu, H.; Wang, Y.; Cao, Y.; Fang, Z.; Lin, T.; Gong, M.; Chen, Y. Catalytic Performance of Acidic zirconium-based Composite Oxides Monolithic Catalyst on Selective Catalytic Reduction of NO_x with NH_3. *Chem. Eng. J.* **2014**, *240*, 62−73.
(36) Yu, J.; Si, Z. C.; Chen, L.; Wu, X. D.; Weng, D. Selective catalytic reduction of NO_x by ammonia over phosphate-containing $Ce_{0.75}Zr_{0.25}O_2$ solids. *Appl. Catal., B* **2015**, *163*, 223−232.
(37) Christou, S. Y.; Alvarez-Galvan, M. C.; Fierro, J. L. G.; Efstathiou, A. M. Suppression of the oxygen storage and release kinetics in $Ce_{0.5}Zr_{0.5}O_2$ induced by P, Ca and Zn chemical poisoning. *Appl. Catal., B* **2011**, *106*, 103−113.
(38) Li, X. L.; Li, Y. H. Molybdenum Modified $CeAlO_x$ Catalyst for the Selective Catalytic Reduction of NO with NH_3. *J. Mol. Catal. A: Chem.* **2014**, *386*, 69−77.
(39) Wu, Z. B.; Jiang, B. Q.; Liu, Y.; Wang, H. Q.; Jin, R. B. DRIFT Study of Manganese/Titania-based Catalysts for Low-temperature Selective Catalytic Reduction of NO with NH_3. *Environ. Sci. Technol.* **2007**, *41*, 5812−5817.
(40) Topsoe, N. Y. Mechanism of the Selective Catalytic Reduction of Nitric Oxide by Ammonia Elucidated by in situ on-line Fourier Transform Infrared Spectroscopy. *Science* **1994**, *265*, 1217−1219.
(41) Chen, L.; Li, J. H.; Ge, M. F.; Ma, L.; Chang, H. Z. Mechanism of Selective Catalytic Reduction of NO_x with NH_3 over CeO_2−WO_3 Catalysts. *Chin. J. Catal* **2011**, *32*, 836−841.
(42) Jiang, B. Q.; Li, Z. G.; Lee, S. C. Mechanism Study of the Promotional Effect of O_2 on Low-Temperature SCR Reaction on Fe−Mn/TiO_2 by DRIFT. *Chem. Eng. J.* **2013**, *225*, 52−58.

DOI: 10.1021/acsami.5b00636
ACS Appl. Mater. Interfaces 2015, 7, 9497−9506

(43) Chen, L.; Li, J.; Ge, M. DRIFT Study on Cerium−Tungsten/Titania Catalyst for Selective Catalytic Reduction of NO_x with NH_3. *Environ. Sci. Technol.* **2010**, *44*, 9590−9596.
(44) Liu, F. D.; Asakura, K.; He, H.; Liu, Y. C.; Shan, W. P.; Shi, X. Y.; Zhang, C. B. Influence of Calcination Temperature on Iron Titanate catalyst for the Selective Catalytic Reduction of NO_x with NH_3. *Catal. Today* **2011**, *164*, 520−527.
(45) Liu, F. D.; Shan, W. P.; Lian, Z. H.; Xie, L. J.; Yang, W. W.; He, H. Novel $MnWO_x$ Catalyst with Remarkable Performance for Low Temperature NH_3-SCR of NO_x. *Catal. Sci. Technol.* **2013**, *3*, 2699−2707.
(46) Tsyntsarski, B.; Avreyska, V.; Kolev, H.; Marinova, T.; Klissurski, D.; Hadjiivanov, K. FT-IR Study of the Nature and Reactivity of Surface NO_x Compounds formed after NO Adsorption and NO + O_2 Coadsorption on Zirconia- and Sulfated Zirconia-supported Cobalt. *J. Mol. Catal. A: Chem.* **2003**, *193*, 139−149.
(47) Zhang, R.; Zhong, Q.; Zhao, W.; Yu, L.; Qu, H. Promotional effect of fluorine on the selective catalytic reduction of NO with NH_3 over CeO_2−TiO_2 catalyst at low temperature. *Appl. Surf. Sci.* **2014**, *289*, 237−244.

DOI: 10.1021/acsami.5b00636
ACS Appl. Mater. Interfaces 2015, 7, 9497−9506